

“© 2015 IEEE. Personal use of this material is permitted. Permission from IEEE must be obtained for all other uses, in any current or future media, including reprinting/republishing this material for advertising or promotional purposes, creating new collective works, for resale or redistribution to servers or lists, or reuse of any copyrighted component of this work in other works.”

Massive Hybrid Antenna Array for Millimeter Wave Cellular Communications

Jian A. Zhang, *Senior Member, IEEE*, Xiaojing Huang, *Senior Member, IEEE*,

Val Dyadyuk, *Member, IEEE*, and Y. Jay Guo, *Fellow, IEEE*

ABSTRACT:

A massive hybrid array consists of multiple analog subarrays, with each subarray having its digital processing chain. It offers the potential advantage of balancing cost and performance for massive arrays and therefore serves as an attractive solution for future millimeter wave (mm-wave) cellular communications. On one hand, using beamforming analog subarrays such as phased arrays, the hybrid configuration can effectively collect or distribute signal energy in sparse mm-wave channels. On the other hand, multiple digital chains in the configuration provide multiplexing capability and more beamforming flexibility to the system. In this article, we discuss several important issues and the state-of-the-art development for mm-wave hybrid arrays, such as channel modeling, capacity characterization, applications of various smart antenna techniques for single user and multi-user communications, and practical hardware design. We investigate how the hybrid array architecture and special mm-wave channel property can be exploited to design sub-optimal but practical massive antenna array schemes. We also compare two main types of hybrid arrays, interleaved and localized arrays, and recommend that localized array is a better option in terms of overall performance and hardware feasibility.

Affiliations:

The authors are with the Division of Computational Informatics, CSIRO, Sydney, Australia.

Email address: { Andrew.Zhang; Xiaojing.Huang; Val.Dyadyuk; Jay.Guo}@csiro.au

1. INTRODUCTION

Owing to the large bandwidth available, millimeter wave (mm-wave) radio, particularly that operating in the frequency range of 28 to 90 GHz, has been considered as a very promising candidate for 5G cellular communications [1]. Compared to microwave systems, however, the propagation attenuation of mm-wave is much higher and the radiation power achievable is much lower. Hence it is necessary to use high-directivity antennas to ensure that sufficiently high signal power can be received for successful signal detection. Furthermore, to support mobile users and users at different locations, mm-wave radio needs to use steerable directional antennas or configurable antenna arrays. Thanks to the small wavelength of mm-wave, it is feasible to accommodate a large number of antenna elements in a physically limited space. Hence, for mm-wave cellular communications, massive antenna array is becoming a promising proposition.

Unfortunately, a full digital array, i.e., using a radio frequency (RF) front-end and digital baseband for each antenna, is very costly although it provides full capacity and flexibility [2]. Full digital mm-wave massive array is also impractical due to the tight space constraints, that is, the small separation of array elements leaves little room at the back of the array to accommodate all RF chains and for connecting them to the baseband processors. A hybrid array, which consists of multiple analog subarrays with each subarray having its own digital chain, turns out to be a more feasible solution [5, 13]. It can not only provide a significant saving on cost and complexity, but also achieve comparable performance in many applications due to the special mm-wave propagation features.

One important feature of mm-wave signal propagation is multipath sparsity in both temporal and spatial domains. Such sparsity is mainly caused by the following two propagation phenomena: 1) the energy of reflected mm-wave signal decreases very quickly and only multipaths with one or two reflections carry notable power; and 2) diffraction becomes less prominent due to a smaller radius of Fresnel zone. Therefore only a few multipath signals arrive in some concentrated directions and the non-line-of-sight (NLOS) component has much lower power compared to the LOS component, as reported in [1].

Thanks to the multipath sparsity, a massive hybrid array becomes an attractive solution for mm-wave communications. On one hand, using beamforming analog subarrays such as phased arrays, one can effectively collect or distribute signal energy by adjusting the phase of the received or transmitted signal. On the other hand, using individual digital processing chain for each subarray, one can add multiplexing capability to the system. At the same time, it provides significant flexibility in beamforming design and improves the system's capability in dealing with multipath and multi-user interference (MUI).

Undoubtedly, massive hybrid array for mm-wave communications faces many challenging design problems due to both the special signal propagation property and large degree of freedom provided by the hybrid array structure. In this article, we will offer a comprehensive review of the state-of-the-art development for mm-wave massive hybrid array, highlighting research challenges and discussing potential

solutions. We will also investigate how to exploit the special features of the mm-wave hybrid array in signal processing to optimize beamforming algorithm design and reduce algorithm complexity.

2. MASSIVE HYBRID ARRAY ARCHITECTURES

Figure 1(a) shows the architecture of a hybrid array, where the whole array is divided into many subarrays. Each subarray is an analog array, consisting of antennas connected with analogue adjustable phase shifters in the RF chain. Each subarray is connected to a baseband processor via a digital-to-analog convertor (DAC) in the transmitter or an analog-to-digital convertor (ADC) in the receiver. Note that the signal at each antenna element of a subarray is weighted by a discrete phase shifting value from a *quantized value set* of which the size is typically represented through the number of quantization bits. For example, 3-bit quantization means 8 discrete values uniformly distributed over $[-\pi, \pi]$. The signals from all the subarrays are interconnected and can be processed centrally in the baseband processor, where spatial precoding/decoding and other baseband processing can be implemented. In the simplest case, the signals to DACs or from ADCs are weighted by complex values, which are known as *digital beamforming*. For convenience, we denote an array with M subarrays and N antenna elements in each subarray as an $N \times M$ array. Typically, N is larger than M such that high antenna gain can be achieved at lower cost. The distance between corresponding elements in adjacent subarrays is called *subarray spacing*.

Depending on the topology of subarrays, we can classify the hybrid array to two types of regular configurations: Interleaved and localized arrays, as illustrated in Fig. 1(b) for a 16×4 uniform square array. In an interleaved array, antenna elements in each subarray scatter uniformly over the whole array; while in a localized array, they are adjacent to each other. These two types of arrays have different properties and suit different applications. A comparison of these two arrays is summarized in Table 1, and detailed analysis is provided throughout the article.

The phase shifting values in the hybrid array can be chosen flexibly to optimize the performance. Conventionally, an analog phased array uses integer multiples of a fixed value for its phase shifters, based on the signal direction. This is effective when signals concentrate in one direction. To fully exploit the potential of the hybrid array, however, it is proposed to allow phase shifting values to be chosen arbitrarily from the quantized value set. This implies that each subarray may form multiple simultaneous beams instead of the traditional single beam in the phased array applications.

3. EQUIVALENT CHANNEL

An equivalent array channel model includes three components: the coupling effect, the single antenna element response (which is assumed to be omni-directional here) and array correlation, and the propagation channel. The equivalent channel matrix can be represented as the product of three matrixes attributing to these components. There are some special issues in channel modeling in the context of mm-wave massive hybrid array, where the large and tightly-packed antenna arrays lead to high levels of

coupling correlation and subarray spatial correlation, and the LOS or near-LOS propagation leads to limited spatial selectivity and scattering.

3.1 MUTUAL COUPLING EFFECTS

The electromagnetic (EM) characteristics of antenna elements can be mutually influenced particularly when they are close to each other. Such effect is called mutual coupling, which introduces *coupling correlation* between neighbouring antenna elements. The effect of mutual coupling can be evaluated by multiplying a coupling matrix to the channel matrix [3, 4]. Therefore in general, it introduces more correlation into the channel matrix, and has a negative influence on many aspects of the array performance, such as the angle of arrival (AoA) resolution capability, array gain, and system capacity. A good overview on these impacts and the mitigation approaches is given in [3]. Surprisingly, mutual coupling is also reported to be advantageous in some cases [3]. For example, the presence of coupling can improve the convergence of adaptive array algorithms, and it may increase channel capacity in dense array systems by reducing the correlation.

So far, there is little published systematic work on characterizing the coupling effect in mm-wave massive array. Some preliminary results on the performance degradation caused by mutual coupling are presented in [4, 5]. However, overly simple mutual coupling models are used and the results may deviate largely from practical situations. Establishing practical coupling models for typical mm-wave arrays is very important for assessing the overall system performance and the effectiveness of mitigation techniques.

3.2 SUBARRAY SPATIAL CORRELATION

In addition to the coupling correlation, we use *subarray spatial correlation* to characterize the similarity of the signals received at different subarrays, considering multiple signals arriving at different angles. Such signals can be multipath signals from a single source, or signals from multiple sources. Subarray spatial correlation is closely related to the capability of a hybrid array on separating signals with close AoAs, and achieving spatial diversity and multiplexing.

Since the output of each subarray is a sum of N signals, the subarray spatial correlation is also affected by the phase shifting values, in addition to the conventional parameters such as element and subarray spacing. The output signals at different subarrays can become strongly uncorrelated even for two signals with close AoAs due to different phase shifting operations. However, it is noted that for a single signal or signals with the same AoA and channel coefficients, the outputs of two subarrays, even when they are widely separated, are still strongly correlated.

Figure 2 demonstrates an example of the subarray spatial correlation for localized and interleaved 4x4 uniform linear arrays (ULAs). As a comparison, the spatial correlation for a full digital array is also plotted. Both correlations are computed considering multiple signals arriving at a small range of angles. The signal AoA follows a truncated Gaussian distribution [6] with mean of 30 degree and variance of 5 degree. When

using aligned beams, the localized array has the same spatial correlation with the full digital array, and localized array shows lower correlation. When the analog phase shifting values are randomly chosen, it is possible to achieve lower correlation, compared to the aligned beam case.

3.3 PROPAGATION CHANNEL

The channel measurement campaigns for mm-wave have mainly been focused on characterizing the pathloss of LOS propagation. Recently, some results have also been reported for NLOS propagation for lower mm-wave band such as the 38 GHz band in [1]. According to [1], the mean of the root mean squared (RMS) delay spread is approximately 1 ns in the LOS case and 12 ns in the NLOS case. Given that the bandwidth of the sounding signal is 400MHz, such delay spreads correspond to 1 and 5 resolvable multipath taps, respectively. It is also observed in [1] that NLOS signals arrive at 2 major angles spaced at about 90 degree. These results confirm the validness of the channel sparsity assumption widely used in the mm-wave literature.

Typical mm-wave multipath channel models reflecting such channel sparsity include the temporal cluster multipath model used in, e.g., [7, 8, 9] and the spatial “double direction impulse response” model used in, e.g., [10]. These models are independent of the antenna array, and can be configured flexibly to represent propagation channels with a limited number of multipath signals.

4. SMART ANTENNA TECHNIQUES

A hybrid antenna array enables various smart-antenna techniques, such as pure beamforming (spatial discrimination and diversity), MIMO (spatial multiplexing) and spatial division multiple access (SDMA). As mentioned before, the mm-wave propagation channels are LOS or near-LOS, which is very different to conventional microwave channels for land mobile communications. This difference, together with the large number of antennas and the hybrid array architecture, motivates the adoption of many new signal processing and optimization techniques. For example, channels without rich scattering drives new design for MIMO, such as LOS-MIMO; SDMA becomes more preferable because it can exploit the channel independence between different users; It is also possible to apply rigid mathematical tools based on beamforming to design MIMO and SDMA systems, instead of relying on channel statistics.

Because of these new features and practical constraints such as the coarse quantization of phase shift, sub-optimal designing techniques are typically adopted, such as 1) Approximating and simplifying optimization functions [9, 10]; 2) Separating transmit precoding and receive equalizer design [8, 9]; and 3) Separating analog and digital beamforming design [7]. Next, we will review some smart antenna techniques, focusing on inspecting how these sub-optimal techniques are applied to simplify system design.

4.1 PURE BEAMFORMING AND AoA ESTIMATION

Here pure beamforming is referred to as the generation of single or multiple beams to achieve spatial discrimination and diversity, and mitigate MUI for a user of interest. It typically involves directly or indirectly estimating AoA of the incident signals and generating beamforming vectors based on the estimates.

AoA estimation in hybrid arrays is quite different from those well-studied ones in either a full analog or digital array. A full analog array generally uses beam scanning to search the AoA, while a full digital array can estimate it in one step using, e.g., spectrum analysis techniques. For a hybrid array, existing algorithms need to be adapted to the special architecture and to different subarray configurations. The AoA estimation algorithms for a hybrid array typically need to be implemented recursively between digital and analog parts. This is because low accuracy AoA estimate leads to low analog beamforming gain and SNR at the digital branches, which results in inaccurate AoA estimation. Hence AoA estimation can only be improved recursively by updating analog beamforming weights with latest estimated AoA values [5].

For estimating a single AoA value, one technique is to exploit the constant phase difference between corresponding elements in two neighbouring subarrays, as proposed in [10], where a differential beam tracking (DBT) algorithm and a differential beam search (DBS) algorithm are proposed for interleaved and localized arrays, respectively. Exploiting phase difference not only removes the necessity of a known reference signal or signal synchronization, but also leads to a Doppler resilient solution. The need for two different algorithms is mainly due to the phase ambiguity problem in the localized configuration. DBS can remove the phase ambiguity, at the cost of increased complexity and reduced convergence speed. To avoid the searching process in DBS, a frequency-domain AoA algorithm is proposed in [5], where the frequency dependent property of a wideband array and the mutual coupling effect are also considered and mitigated. Extension of these algorithms to a near-LOS channel or a multiple beam scenario is yet to be investigated.

It is interesting to note that single localized and interleaved subarrays have different beam patterns but the hybrid arrays have the same pattern when the same digital beamforming vector is used, as demonstrated in Fig. 3. The figure clearly shows the difference between the beam patterns of the two individual subarrays, and the similarity of the two array patterns. The larger grating lobe in the interleaved subarray is suppressed in the array pattern, and the localized subarray does not have grating lobe but has wider beamwidth, which is also reduced significantly in the hybrid array. The beam pattern suggests that interleaved arrays have narrower beamwidth and is more suitable for generating multi-beam for SDMA applications, while localized arrays can better support systems with relatively larger AoA.

4.2 SINGLE USER MIMO

Due to the multipath sparsity, the channel propagation matrix can be near-singular and conventional MIMO capacity will degrade significantly. One alternative approach is to use LOS-MIMO, which relies on careful placement of transmit and receive antennas.

The criterion of antenna placement in a hybrid array is different to that in a full digital array for LOS-MIMO. For a full digital array, the LoS MIMO capacity depends on the orientation of transmit and receive

arrays, their distance R , the element spacing and the number of antenna elements, as presented in [12]. For an mm-wave system with carrier frequency 38 GHz, two parallel uniform linear arrays (ULAs) of 16 elements, and $R=500$ meters, the system capacity is maximized when the element spacing is about 0.5 meter (approximately 63 wavelengths). For a hybrid array, the data symbols are only modulated to digital chains and hence channel independence is only required between different subarrays to maximize the channel capacity. In this case, the beamwidth decreases and the spatial resolvability increases linearly with the increasing of antenna numbers in a subarray. The capacity accordingly becomes closely related to the subarray configurations. Capacity optimization for hybrid arrays remains as a challenging open problem, especially when considering the constraints on discrete phase shifting values.

In Fig. 4, we show an example of the capacity for two parallel 8x4 and 4x4 ULA arrays. The capacity is computed without applying water-filling power optimization. Fig. 4(a) demonstrates how the capacity is affected by antenna element spacing. The capacity upper bound corresponds to the eigen-beamforming. It can only be approached but cannot be achieved by a hybrid array as analog subarrays can only choose discrete phase shifting values. The capacity curves for both interleaved and localized arrays are obtained when all-zero phase shifting values are used, which correspond to the AoA. We have several interesting observations from the figure: 1) The capacity upper bound, as well as the capacity of localized array, are convex functions of the element spacing. They reach the maximum at about 15.75 and 31.5 wavelengths for 8x4 and 4x4 arrays, which are $\frac{1}{4}$ and $\frac{1}{2}$ of the element spacing (61 wavelengths) when the capacity of a full digital array is maximized; 2) For a practical array size, the hybrid array achieves capacity very close to the upper bound and the capacity of full digital arrays; and 3) Interleaved array achieves much lower capacity compared to localized array. Fig. 4(b) demonstrates how the capacity changes with a varying ratio between subarray spacing and element spacing for a given total array size. It can be seen that 1) capacity increases with increasing subarray spacing and the increase can be very significant compared to the uniform spacing case in Fig. 4(a); 2) The gap between the upper bound and the practically achievable one is largely reduced with increased subarray spacing. This is because the subarray correlation is largely reduced with well separated subarrays. Hence using different spacing for inter- and intra- subarrays can be an efficient way of increasing LOS-MIMO capacity, particularly when considering the practical maximal element spacing of a few wavelengths, which is required to maintain the phase shift tolerance in the combining networks. Many of the observations from Fig. 4 are yet to be analytically characterized and generalized.

Applications of the LOS-MIMO, however, may be limited due to the many constraints it requires, for example, fixed link range and the existence of a LoS path. Therefore, single user MIMO is a less attractive option in mm-wave cellular systems where mobile users need to be supported.

Maximization of the MIMO capacity for the hybrid array in a sparse but non-LOS channel is more complex and hence sub-optimal solutions are sought instead. For example, the two aforementioned sub-optimal design techniques, function approximation and transmitter-receiver

separation, are used in [8, 9], where the optimization metric, the system mutual information, is simplified by separating transmit and receive beamforming and exploiting the channel sparsity. The sparse-scattering structure of mm-wave channels is also exploited to formulate the transmit precoder as a simultaneous sparse approximation problem. This sparse precoding approach is then extended to the receiver-side processing based on hybrid minimum mean-square error (MMSE) combining.

4.3 SDMA

Together with user scheduling, SDMA may be realized simply through beamforming. That is, each subarray only communicates to one user, one user can be served by multiple subarrays, and different users are largely separated in directions and can be served by different subarrays. Such a scheme will be effective when the number of users is sufficiently large, although a qualitative analysis is not available yet. In other cases, this scheme becomes sub-optimal but can greatly simplify system design. Under this setup, precoding and equalization can be used to mitigate MUI, as investigated in [7]. In that work, considering MUI, the signal-to-interference and noise ratio (SINR) is used as a metric and the beamforming design is formulated as a SINR constrained power minimization problem. It is further simplified as a semidefinite programming problem by assuming a large K-factor Rician channels based on channel sparsity and dominating LOS propagation.

A more advanced and complex beamformer design has been investigated by considering more general cases where cross-subarray modulation is applied. That is, different users' signals are precoded and mapped to multiple subarrays, and each subarray will form multiple beams pointing at multiple users. These techniques largely exploit channel sparsity to simplify beamformer design. For example, the optimization metric, such as the capacity or mutual information of a hybrid array system, is generally a non-convex function under the constraints of analog phase shifters. To make the optimization problem tractable, approximation is applied to simplify the metric by exploiting large number of antennas, the channel sparsity and the high correlation of channel matrix.

Using the second-order channel statistics to simplify beamformer design is demonstrated in [10], where joint spatial division and multiplexing (JSDM) is proposed for mm-wave hybrid arrays. The JSDM scheme first partitions users with similar covariance channel matrixes into the same group, and then determine the spatial division pre-beamformer and the multi-user MIMO (MU-MIMO) precoder for each group. The pre-beamformer is determined according to the covariance matrix and hence does not require real-time channel feedback. The MU-MIMO precoder is determined by using instantaneous channel values, which are not difficult to obtain thanks to the considerable array dimension reduction after the pre-beamforming. In a hybrid array, the pre-beamforming may be implemented within the analog subarray, while MU-MIMO precoding is through digital weighting.

4.4 PHASE QUANTIZATION AND DELTA-SIGMA SPATIAL SAMPLING

In analog beamforming, typically 3 to 6 bits phase shifters, corresponding to 8 to 64 discrete phase shifting values, are required. Depending on the RF architecture as to be discussed later, it can be very expensive to implement such phase shifters in a massive array. Using 1 or 2-bit phase shifters directly can lead to reduced beamforming resolution capability and cause increased pointing error and relatively high sidelobes, especially for smaller scanning angle.

Two classes of conventional techniques can be used to mitigate the coarse quantization impact mainly through using different phase shifter values in neighboring antenna elements. The first class of techniques can be termed as *phase determination algorithms* which compute the phase shifting values in a deterministic way. These techniques require no extra hardware, but their computational complexity is high as phase shifting values need to be optimized under multiple constraints instead of signal AoA only. For example, robust beamforming design under the phase quantization error is investigated in [7], where a robust formulation based on the S-procedure is first established to characterize and combat phase uncertainty using SNR maximization, and an extended nonlinear formulation is then proposed to solve the beamforming vectors iteratively. The second class of techniques can be called as *phase randomization algorithms* which introduce (small) random phase shifting values to each array element. Such phase shifting values can be added to the quantized ones obtained from the AoA estimates. These techniques have lower computational complexity but require extra hardware for the random phase shifters. Introducing the random phase perturbation by, e.g., using transmission lines of different length can be an implementation challenge in line routing and phase value control in actual massive array manufacturing. For high speed mm-wave systems supporting mobile users, the phase randomization algorithms are more suitable as they have less computational time and the beam scanning can perform faster.

Recently, a Delta-Sigma phased array is proposed in [4] to overcome the coarse quantization problem. The technique extends the well-known time-domain Delta-Sigma ADCs to the spatial domain. It applies sub-half-wavelength element spacing in uniform arrays, and steers beam pattern quantization error into the so-called invisible region of space, while leaving the intended pattern throughout the (visible) area of interest. Furthermore, it is found in [4] that the Delta-Sigma phased array can replicate the beam pattern of arbitrary amplitudes as well as arbitrary phases while in fact the amplitude is uniform for every element. This implies that it can completely eliminate the need for individual amplitude control. Hence the Delta-Sigma phased array allows for tradeoffs between complex phase shifter design and dense antenna implementations, which suits a massive array very well. However, extension of the Delta-Sigma phased array to a hybrid array is not straightforward, particularly for MIMO and SDMA applications, where multiple signals with different AoAs need special processing in the framework.

4.5 HARDWARE: RF AND PHASE SHIFTER

Ideally, a high-gain pencil beam is generated by a true time delay at each element that compensates exactly for the free-space propagation delay. Developing a low-loss, linear delay line directly at mm-wave frequencies is very challenging. Some of the promising newer technologies for implementing broadband true time delay include switched-length transmission lines using RF micro-electro-mechanical (MEMS) switches and variable velocity transmission lines based on ferroelectric materials. However, many problems such as reliability and frequency-dependent loss need to be overcome.

Equivalent delays can also be more practically implemented by phase-shifters in the RF, intermediate frequency (IF) or local oscillator (LO) channels. Several possible receive RF chain architectures are shown in Fig 5. Architectures of the transmit RF chain is very similar with a reverse signal flow and the low noise amplifier (LNA) replaced with power amplifier. All the illustrated architectures use an optional variable attenuator at IF, which can be used for compensating the conversion gain variations and loss in the combining network and calibration of the analogue subarray. This also adds finite magnitude adjustment capability to analog subarrays, which has hardly been considered in the literature of signal processing for the mm-wave hybrid array.

Option in Fig 5(a) could be utilised in arrays where an LNA is shared between several antenna elements (corporate power combining/splitting). A modification of this architecture, where the receiver sensitivity can be improved by placing the phase shifter after the LNA, is shown in Fig 5(b). This option can be implemented either using a shared frequency converter (with individual RF chains combined at the input to the mixer) or individual frequency conversion and combining at the IF. However, high-resolution phase shifters with low insertion loss and phase errors are not available for upper mm-wave bands (>50 GHz) at present. Fig. 5(c) and (d) show more practical (at present) configurations with commercially available 4-6-bit phase shifters implemented at the IF and LO circuits respectively. The latter option is particularly attractive since the devices in the LO path are typically operated in saturation, and variable loss with phase shift is not a problem.

RF chains shown in Fig 5 (a)-(d) can be combined in various ways into the antenna array. However, integration of an individual RF chain behind the antenna array element is not feasible as the physical size of the component in existing semiconductor technologies exceeds space constraints. Instead, it is possible to integrate all the RF chains for a subarray behind it as has been done in [13, 14] for a 16-element localized square subarray. Because of such subarray-based RF integration, routing for interleaved array becomes very challenging.

Recently, beamspace MIMO [15] is proposed for mm-wave hybrid arrays based on the use of a high-resolution discrete lens array (DLA) for analog beamforming. The DLA exploits electronic lens to redirect and focus signals and is very different to conventional phase shifters as discussed above. It can provide nearly continuous phase shift. Both hardware design and signal processing based on DLA are interesting areas to be explored.

5. CONCLUSIONS

We have reviewed several important problems in mm-wave massive hybrid array, such as channel modeling, capacity, applications of various smart antenna techniques, and hardware implementation. We have demonstrated how sub-optimal designing techniques exploiting the array and channel properties can be efficiently applied. We have also shown that localized array is a better option in terms of overall performance and hardware feasibility. Mm-wave massive hybrid array can achieve great balance between performance and cost, and is very promising for next generation cellular communications.

REFERENCE

1. T.S. Rappaport, S. Sun, R. Mayzus, H. Zhao, Y. Azar, K. Wang; G.N. Wong, J.K. Schulz, M. Samimi, F. Gutierrez, "Millimeter Wave Mobile Communications for 5G Cellular: It Will Work!," *Access, IEEE*, vol.1, no., pp.335-349, 2013
2. E. Torkildson, B. Ananthasubramaniam, U. Madhow, and M. Rodwell, "Millimeter-wave MIMO: Wireless Links at Optical Speeds", *Proc. Of 44th Allerton Conf. on Communication, Control and Computing*, Monticello, Illinois, Sep. 2006
3. S. Hema, H. L. Sneha, and R. M. Jha, "Mutual Coupling in Phased Arrays: A Review," *International Journal of Antennas and Propagation*, vol. 2013, Article ID 348123, 23 pages, 2013.
4. J.D. Krieger, C. Yeang, G.W. Wornell, "Dense Delta-Sigma Phased Arrays," *Antennas and Propagation, IEEE Transactions on*, vol.61, no.4, pp.1825-1837, April 2013
5. X. Huang and Y. J. Guo, "Frequency-Domain AoA Estimation and Beamforming with Wideband Hybrid Arrays," *IEEE Transactions on Wireless Communications*, Vol. 10, No. 8, pp.2543-2553, August 2011
6. Jiann-An Tsai, R. Michael Buehrer, and B. D. Woerner, "BER Performance of a Uniform Circular Array Versus a Uniform Linear Array in a Mobile Radio Environment", *IEEE Transactions on Wireless Communications*, Vol. 3(3), pp. 695-2004, May 2004
7. S. Wu; L. Chiu; K. Lin; T. Chang, "Robust Hybrid Beamforming with Phased Antenna Arrays for Downlink SDMA in Indoor 60 GHz Channels," *Wireless Communications, IEEE Transactions on*, vol.12, no.9, pp.4542-4557, September 2013
8. O. El Ayach, S. Abu-Surra, S. Rajagopal, Z. Pi, and R. W. Heath, Jr., "Spatially Sparse Precoding in Millimeter Wave MIMO Systems," submitted to *IEEE Trans. on Wireless*, May 2013.
9. A. Alkhateeb, O. El Ayach, G. Leus, R.W. Heath Jr, "Hybrid Precoding for Millimeter Wave Cellular Systems with Partial Channel Knowledge," *Proc. of Information Theory and Applications (ITA) Workshop*, 2013
10. A. Adhikary, J. Nam, J.-Y. Ahn, and G. Caire, "Joint spatial division and multiplexing: The large-scale array regime," *Information Theory, IEEE Transactions on*, vol. 59, no. 10, pp. 6441–6463, 2013.

11. X. Huang, Y. J. Guo and J. Bunton, "A Hybrid Adaptive Antenna Array", IEEE Transactions on Wireless Communications, Issue 5, Vol. 9, pp1770-1779, 2010.
12. I. Sarris and A. R. Nix, "Design and Performance Assessment of High-Capacity MIMO Architectures in the Presence of a Line-of-Sight Component", IEEE Trans. Vehicular Tech., Vol 56 (4), pp. 2194-2202, July 2007
13. Y. J. Guo, X. Huang and V. Dyadyuk, "A Hybrid Adaptive Antenna Array for Long Rang mm-Wave Communications," IEEE Antennas and Propagation Magazine, Vol. 54, Issue 2, pp. 271 – 282, April 2012.
14. V. Dyadyuk, X. Huang, L. Stokes, J. Pathikulangara, A.R. Weily, N. Nikolic, J.D. Bunton, Y. J. Guo, "Adaptive Antenna Arrays for Ad-Hoc Millimetre-Wave Wireless Communications", In: M. Khatib, ed. Advanced Trends in Wireless Communications, Chapt. 6, pp.93-116, InTech, Feb. 2011.
15. J. Brady, N. Behdad, A.M. Sayeed, "Beamspace MIMO for Millimeter-Wave Communications: System Architecture, Modeling, Analysis, and Measurements," Antennas and Propagation, IEEE Transactions on , vol.61, no.7, pp.3814-3827, July 2013

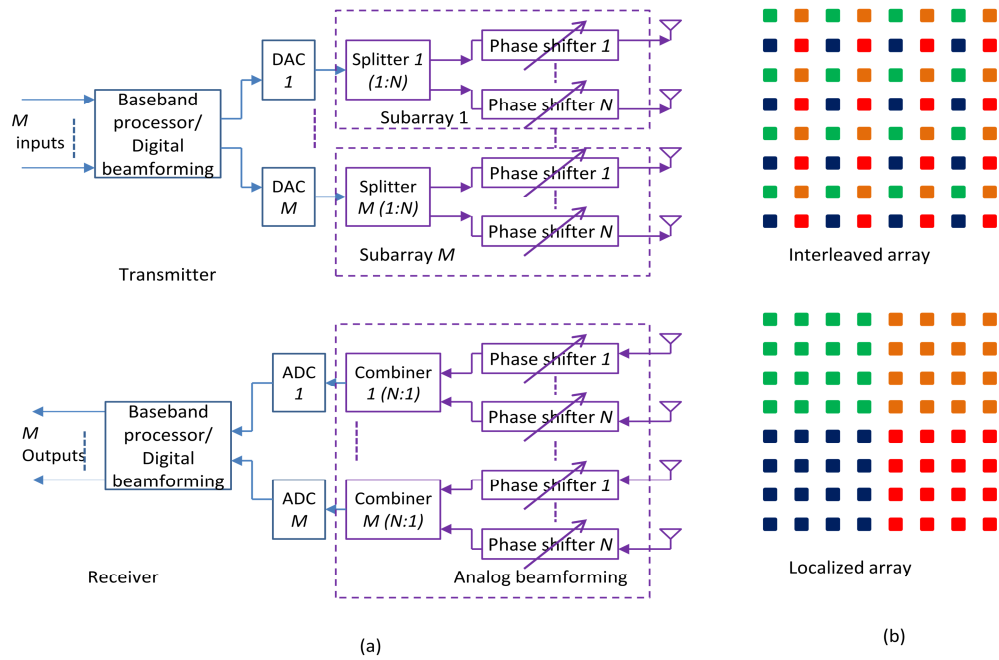


FIGURE 1 (a) Hybrid array architecture for a transmitter and receiver and (b) two types of array configurations in hybrid uniform square arrays: Interleaved (upper) and localized (bottom) configurations. For simplicity, RF chain of the analogue subarray in Fig 1(a) has been depicted as a single component – phase shifter.

TABLE 1 Comparison of Interleaved and Localized arrays. Texts in blue and red are for advantages and disadvantages, respectively.

	Subarray Beam Width	Subarray Grating Lobe	Complexity of AoA Estimation	LOS-MIMO Capacity for given array size	Hardware Implemen- tation	More Suitable Applications
Interleaved Array	Narrow	Large	Lower	Smaller	Challenging	Pure beamforming, SDMA
Localized Array	Wide	Small	Higher	Larger	Practical	LOS-MIMO SDMA, MIMO

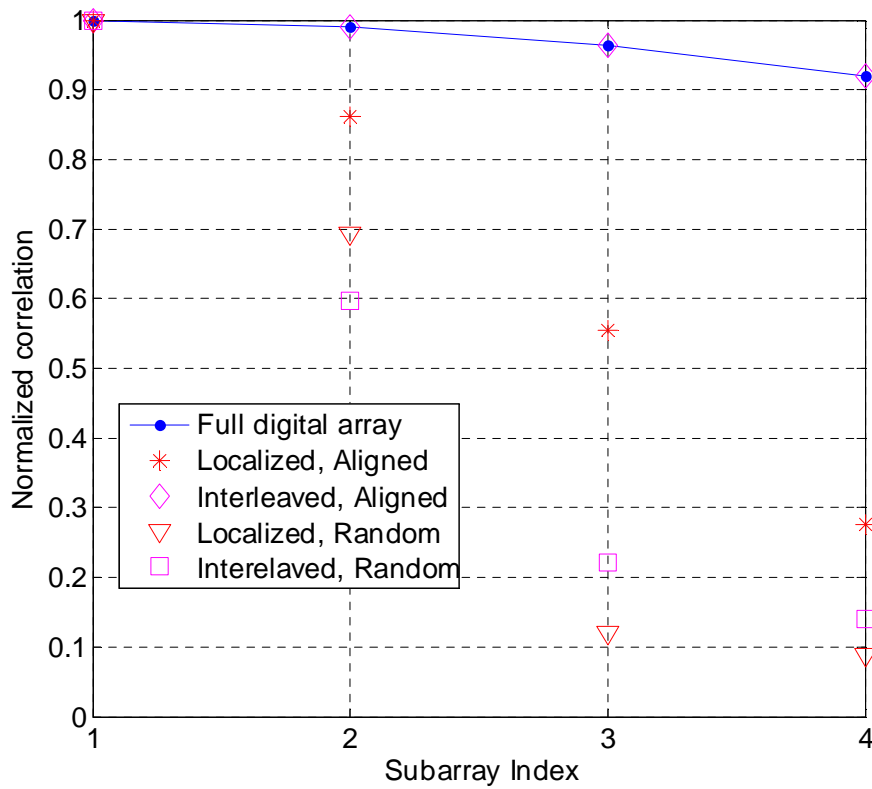


FIGURE 2. NORMALIZED Spatial correlation between the first subarray and its neighbors for localized and interleaved 4x4 ULA with half wavelength element spacing. For the full digital array, subarray index is the element index. The phase shifting values in subarrays are chosen 1) randomly (with legend “Random”), and 2) as a beamforming vector with linearly shifted phases corresponding to the AoA (with legend “Aligned”).

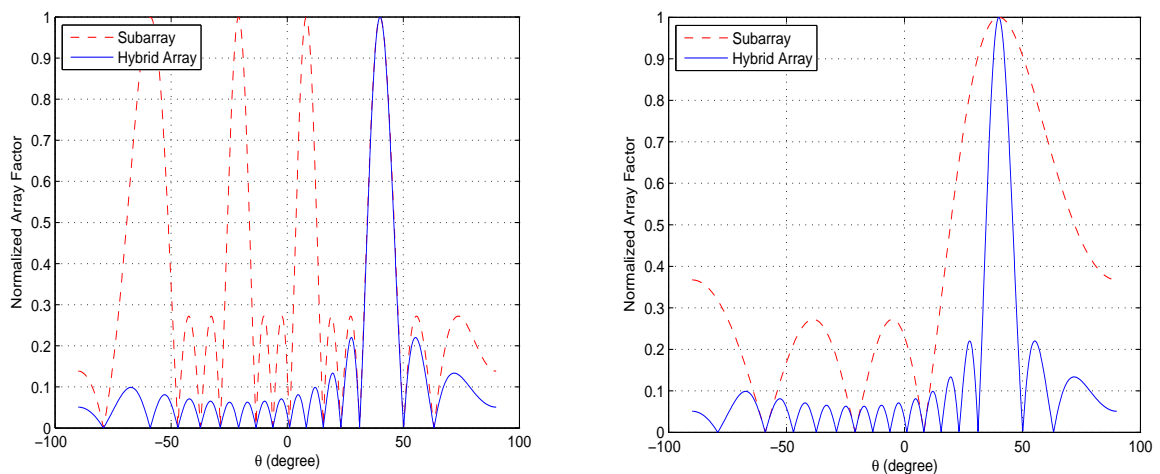


FIGURE 3 Normalized array factor of a uniform 16x16 square hybrid array with square subarrays in the interleaved (left) and localized configuration (right). The beam direction is at zenith angle of 40 degree and azimuth angle of 0 degree. X-axis is for the zenith angle.

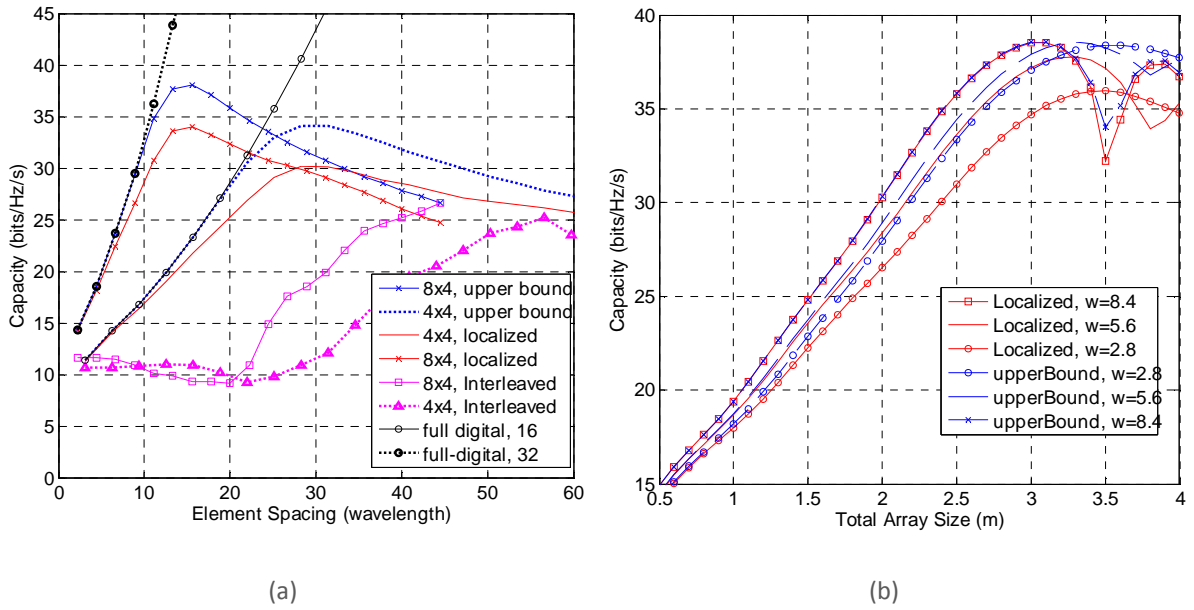


FIGURE 4 Capacity of LOS-MIMO systems for two parallel ULA arrays at an averaged received SNR of 20 dB. (a) Capacity versus uniform element spacing for 4x4 and 8x4 arrays. The two curves with legend “full digital” are for the capacity of full digital arrays with 16 and 32 antennas. The capacity upper bounds are obtained by assuming that analog subarrays can implement eigen-beamforming to convert the channel matrix into a diagonal matrix with non-zero elements corresponding to the 4 largest eigenvalues. (b) Capacity variation with different subarray and element spacing in an 8x4 hybrid array, when the total array size is fixed. The variable w denotes the ratio between the subarray spacing and element spacing. Wavelength is 0.0079m.

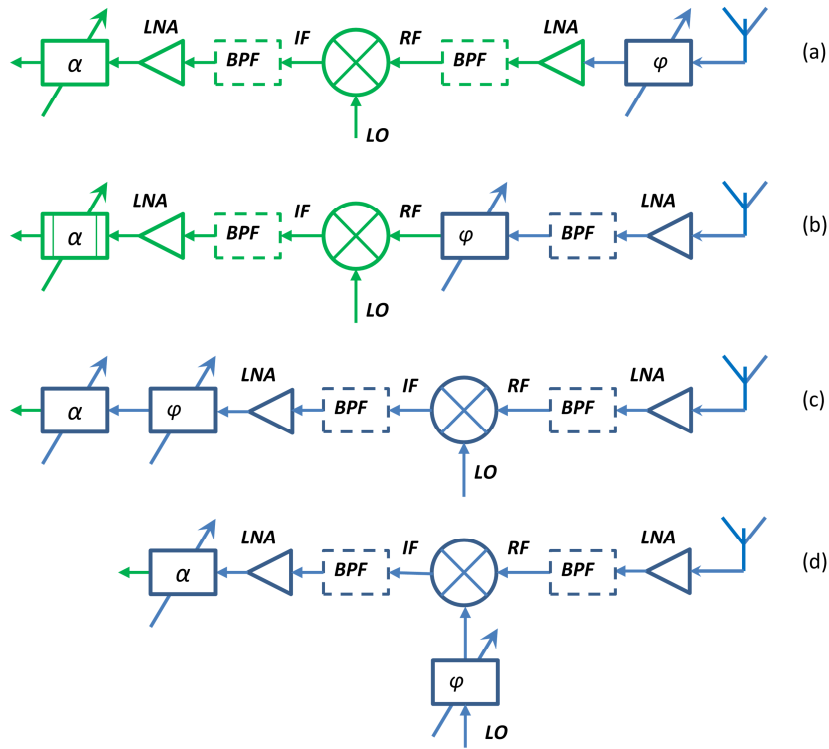


Figure 5 Block diagrams of the receive RF chain associated with each antenna element where the blocks φ and α denote variable phase shifter and magnitude attenuator, respectively. Blocks in green represent those able to be shared by antenna elements in a subarray. (a) Phase shifter φ at the RF before an LNA, (b) Phase shifter at the RF after an LNA, (c) Phase shifter at the IF, (d) Phase shifter at the LO. Band-pass filters (BPF) are required for band limiting and image rejection (in most applications) and are optional for certain applications.